Modeling and Simulation in Science, Engineering and Technology

Series Editor

Nicola Bellomo
Politecnico di Torino
Italy

Advisory Editorial Board

Mathematical Modeling of Biological Systems, Volume II

Epidemiology, Evolution and Ecology, Immunology, Neural Systems and the Brain, and Innovative Mathematical Methods

Andreas Deutsch
Rafael Bravo de la Parra
Rob J. de Boer
Odo Diekmann
Peter Jagers
Eva Kisdi
Mirjam Kretzschmar
Petr Lansky
Hans Metz
Editors

Birkhäuser
Boston • Basel • Berlin

Andreas Deutsch
Center for Information Services
  and High Performance Computing
Technische Universität Dresden
01062 Dresden
Germany

Rafael Bravo de la Parra
Departamento de Matemáticas
Universidad de Alcalá
28871 Alcalá de Henares
Spain

Rob J. de Boer
Department of Theoretical
  Biology
Utrecht University
Padualaan 8
3584 CD Utrecht
The Netherlands

Odo Diekmann
Mathematisch Instituut
Utrecht University
Budapestlaan 6
3584 CH Utrecht
The Netherlands

Peter Jagers
Mathematical Sciences
Chalmers University of Technology
Göteborg University
412 96 Göteborg
Sweden

Eva Kisdi
Department of Mathematics
  and Statistics
University of Helsinki
Gustaf Hällströmin katu 2b
00014 Helsinki
Finland

Mirjam Kretzschmar
Fakultät für Gesundheitswis-
  senschaften
Universität Bielefeld
Universitätsstr. 25
33615 Bielefeld
Germany

Petr Lansky
Institute of Physiology
Academy of Sciences of
  the Czech Republic
Videnska 1083
142 20 Prague 4
Czech Republic

Hans Metz
Section Theoretical
  Evolutionary Biology
Institute of Evolutionary and
  Ecological Sciences
Rijksuniversiteit Leiden
Kaiserstraat 63
2311 GP Leiden
The Netherlands

9 8 7 6 5 4 3 2 1

www.birkhauser.com   (LM/EB)

Preface

This edited volume contains a selection of chapters that are an outgrowth of the European Conference on Mathematical and Theoretical Biology (ECMTB05, Dresden, Germany, July 2005). The peer-reviewed contributions show that mathematical and computational approaches are absolutely essential to solving central problems in the life sciences, ranging from the organizational level of individual cells to the dynamics of whole populations.

The contributions indicate that theoretical and mathematical biology is a diverse and interdisciplinary field, ranging from experimental research linked to mathematical modelling to the development of more abstract mathematical frameworks in which observations about the real world can be interpreted and with which new hypotheses for testing can be generated. Today, much attention is also paid to the development of efficient algorithms for complex computations and visualization, notably in molecular biology and genetics. The field of theoretical and mathematical biology and medicine has profound connections to many current problems of great relevance to society. The medical, industrial, and social interests in its development are in fact undisputable. Insights and predictions from mathematical modelling are used increasingly in decision support in medicine (e.g., immunology and spread of infectious diseases, cancer research, cardiovascular research, neurological research, optimization of medical treatments, imaging), environmental and nature management, climate problems, agriculture and management of natural resources. Fast developments in areas such as biotechnology (e.g., genome projects, genetic modification, tissue engineering) continue to add new focal points of activity to the field. The contributions of this volume capture some of these developments.

The volume contains five parts: epidemiology, evolution and ecology, immunology, neural systems and the brain, and, finally, innovative mathematical methods and education.

Part I deals with epidemiology and contains three chapters.

Smith discusses implications of new malaria vaccines. Recent breakthroughs in malaria vaccines have given new hope that a safe, effective malaria vaccine may be found. In particular, the following epidemiological questions are addressed: 1. What

level of vaccination coverage is required to offset the limitations of an imperfect disease-modifying vaccine? 2. Could the introduction of a low-efficacy malaria vaccine lead to an increase in the number of secondary infections? 3. What characteristics of such a vaccine will have the greatest effect on the outcome? A mathematical model is developed for a disease-modifying malaria vaccine that is given once prior to infection, and the minimum coverage level for disease eradication is established. It is shown that there is a threshold depending on the relative rate of infection, the efficacy of the vaccine, and the duration of infection. Vaccines which reduce the rate and duration of infection will always result in a decrease in secondary infections. More surprisingly, there is a duration "shoulder," such that vaccines that increase the duration of infection slightly will still lead to a decrease in secondary infections, even if the rate of infection is unchanged. Beyond this, the number of secondary infections will increase unless the rate of infection is sufficiently lowered. This is critical for low-efficacy vaccines.

Burie, et al. introduce a model for the invasion of a fungal disease over a vineyard. In particular, the spatiotemporal spreading of a fungal disease over a vineyard is investigated using a SEIR-type model coupled with a set of partial differential equations describing the dispersal of the spores. The model takes into account both short and long range dispersal of spores and growth of the foliar surface. Results of numerical simulations are presented, and a mathematical result for the asymptotic behavior of the solutions is given.

Stollenwerk and Mikolajczyk present an algorithm for parameter estimation in nosocomial infections. Parameter estimation in nosocomial infections poses specific problems for estimation techniques. The mathematical description of the spread of nosocomial infections incorporates transmission as the dynamic part; the outcome is discrete, and the amount of available information is usually small. The authors transfer an estimation technique developed previously for plant epidemics to nosocomial infections and demonstrate its application to a data set related to methicillin-resistant *Staphyloccocus aureus* (MRSA).

Part II focuses on evolution and ecology and consists of eight chapters.

Broom, et al. discuss evolutionarily stable investment in anti-predatory defenses and aposematic signalling. Many species possess defenses (such as toxins) against predator attack which cannot be observed by the predator prior to attack, but which might be beneficial for the predator to avoid. Often, such animals are brightly colored or have some other way of signalling that they are defended (aposematism). In an earlier paper the authors examined the evolution and maintenance of defense and conspicuousness, the brightness of the defense signal, in such prey species using a game theoretic model. Here, they develop the model further, and, in particular, expand on the more theoretical results with examples demonstrating the type of solutions which can occur. The authors categorize eight possible configurations of solution states for simple solutions. Finally, it is shown that there is another class of solutions possible where there is strong between-individual variation in appearance between conspicuous, poorly defended prey, and one example of this complex solution is demonstrated.

Laird, et al. introduce an overview of the Tangled Nature model of evolutionary ecology. The model focuses on the effect of evolution and multiple interactions on

ecological and evolutionary observables. Furthermore, the model is individual based, and ecological structures, such as species, are emergent quantities. The dynamics consists of a simplistic mutation-prone multiplication in which the probability of producing an offspring is determined by the occupancy in genotype space. The macroscopic long-time dynamics is intermittent and exhibits a slow decrease in the macroscopic extinction rate. Ecological quantities such as the species-abundance distribution and the species-area relationship compare qualitatively well with observations, as does the relation between interaction and diversity. The effect of correlations between parents and mutants has been studied, as well as the effect of a conserved resource.

Garay discusses the relative advantage and fundamental theorems of natural selection. According to the tenet of Darwinian selection, a phenotype will spread only if its fitness is greater than the mean fitness of the entire population. It is therefore natural to introduce the notion of relative advantage of a replicator, which is defined as the expected fitness of this replicator minus the average fitness of the entire replicator population. For general replicator dynamics, it is shown that the relative advantage of an offspring population over its parent population is proportional to the variance in fitness. The relationship between the proposed and earlier versions of the fundamental theorem of natural selection is also discussed.

Kon considers competitive exclusion between year-classes in a semelparous biennial population. In particular, competitive exclusion between two reproductively isolated year-classes in the Leslie matrix model for a semelparous biennial population is investigated. The results show that competitive exclusion occurs if competition is more severe between than within year-classes. A criterion is suggested which is applicable even if the model exhibits complex behavior.

Nedorezov, et al. study the impact of winter conditions on the dynamics of an isolated population. In particular, this chapter is devoted to the analysis of single-species population dynamics models with overlapping and nonoverlapping generations. It is assumed that there are no activities of individuals during the winter time (as, for example, is the case for forest insect populations in the boreal zone), and changes in population size at these moments are described with a broken trajectory ("jump down"). Furthermore, it is assumed that the fecundity of individuals is constant and that the quota of individuals surviving winter depends on the within-year population dynamics. The dynamics of the models, which are determined by the influence of winter conditions on the survival of individuals and by the influence of intra-population self-regulative mechanisms, are analyzed. For some particular cases the conditions for population extinction and for stabilization at a nonzero level are determined; it is shown numerically that chaotic regimes exist in some models. In addition, the conditions for the reduction of the models to some well-known discrete models are obtained.

Fuller, et al. consider the topic of planning for biodiversity conservation using stochastic programming. Rapid species extinctions and the loss of other biodiversity features worldwide have prompted the development of a systematic planning framework for the conservation of biodiversity. Limited resources (~ 40 million USD annually) are available for conservation, particularly in the developing countries that contain many of the world's hotspots of species diversity. Thus, conservation planning problems are often represented as mathematical programs in which the objective is to

select sites to serve as conservation areas so that the cost of the plan is as small as possible and adequate habitat is protected for each species. Here, the authors generalize this approach to allow for uncertainty in the planning process. In particular, it is assumed that the species to be protected disperse after the conservation areas are established and that planners cannot anticipate with certainty the species' future locations when selecting the conservation areas. This uncertainty is modeled by including random variables in the mathematical program. The approach is illustrated by designing a network of conservation areas for birds in southern Quebec.

Eberl and Schraft present a diffusion-reaction model of a mixed culture biofilm arising in food safety studies. Bacterial biofilms are communities of microorganisms that develop on interfaces in aqueous environments. The authors formulate a density-dependent diffusion-reaction model for the growth of a dual-species biofilm. Both bacteria respond differently to their environment and develop different types of biofilms: one is a classical aerobic biofilm former that produces the characteristic cluster-and-channel biofilm morphology; the other one also develops under anaerobic conditions and tends to form flat, creeping biofilms. A previously developed nonstandard finite-difference scheme is adapted for computer simulation. In a numerical experiment it is shown how variations of a single parameter (growth rate) can trigger different spatial patterns and organization of the biofilm community.

Iwata, et al. discuss the periodical population dynamics of lottery models with undeveloped seeds. The mechanism that promotes coexistence of species has not been completely clarified yet. The authors propose that the amount of nutrient can be one of the factors that promotes coexistence of species. Plant species have to reproduce seeds to produce descendants. Even if plant species do reproduce seeds, it is not ensured that every seed will bud. The amount of seeds that can bud successfully depends on the amount of nutrient: if the nutrient is scarce, then not every seed can bud, but if the nutrient is rich, then every seed can bud. It is also assumed that the amount of seeds reproduced by one plant individual depends on the amount of nutrient. It is shown that in this situation the population dynamics of plants exhibits a complex behavior, which promotes coexistence of species.

Part III deals with the immune system and has four chapters.

Zanlungo, et al. present an automata-based microscopic model for the clonal expansion process. The model is based on a repertoire of antigens and T lymphocytes interacting via the APC cells which present the antigen peptides. Each cell is represented by an automaton moving randomly on a two-dimensional lattice. This simplified model is used in order to introduce local and spatial considerations in the mathematical models of clonal expansion based on differential equations, and at the same time to attempt an analytical interpretation of the results of computer simulations. Furthermore, a mean field theory is derived, whose results are in good agreement with the solutions of the microscopic model, at least for situations that are not too far from equilibrium. This model may be used as the basis of a more realistic one that could follow the clonal expansion process on a simplified version of the lymphatic network.

Vogel and Behn focus on Th1–Th2 regulation and allergy and present a bifurcation analysis of the nonautonomous system. A previously proposed mathematical model

based on a simplified scheme of Th1–Th2 regulation mediated by the cytokine network which describes the population dynamics of allergen-specific naive T cells, Th1 and Th2 cells, autocrine and cross-suppressive cytokines, and allergen is further investigated. The model provides a theoretical explanation of the switch from a Th2-dominated response to a Th1-dominated response to allergen in allergic individuals as a result of a hyposensitization therapy. The authors focus here on the bifurcation analysis of the nonautonomous dynamical system driven by periodic allergen injections. The stability of the fixed points of a stroboscopic map is investigated. The set of unstable fixed points forms the dynamical separatrix between the regions of Th2-dominated response and Th1-dominated response which is crossed during a successful therapy. The maintenance phase of the therapy holds the system near the stable fixed point of the stroboscobic map.

Schmidtchen and Behn discuss the architecture of randomly evolving idiotypic networks. B lymphocytes express on their surface receptors (antibodies) of a given specificity (idiotype). Crosslinking these receptors by complementary structures, antigens or antibodies, stimulates the lymphocyte. Thus, a large functional network of interacting lymphocytes, the idiotypic network, emerges. Idiotypic networks, conceived by Niels Jerne 30 years ago, experience a renewed interest, e.g., in the context of autoimmune diseases. In a previously proposed minimalistic model, idiotypes are represented by bit strings. The population dynamics of the idiotype clones is reduced to a zero-one scheme. An idiotype survives only if it meets enough but not too many complementary structures. The authors investigate the random evolution of the network towards a highly organized functional architecture which is driven by the influx of new idiotypes, randomly generated in bone marrow. The vertices can be classified into different groups, which are clearly distinguished, e.g., by the mean lifetime of the occupied vertices. They include densely connected core groups and peripheral groups of isolated vertices, resembling the central and peripheral parts of the biological network. The authors have determined the construction principles of the observed patterns and propose a description of their architecture, which is easily transferable to other patterns and applicable to different system sizes.

Sannikova presents an analysis of infectious mortality by means of the individualized risk model. The goal of the work is to describe the mechanism underlying the age-specific increase in death risk related to immunosenescence and to determine the cause-specific hazard rate as a function of immune system characteristics. Therefore, a mathematical model that allows for the estimation of the age-specific risk of death caused by infectious diseases has been developed. The model consists of three parts: (1) a model of immunosenescence, (2) a model of infectious disease, and (3) a model giving the relationship between disease severity and the risk of death. The proposed model makes it possible to analyze age-specific mortality from infectious diseases and to predict future changes in mortality due to public health activity. At the same time it can be used for individualized risk assessment.

Part IV deals with neural systems and the brain and includes nine chapters.

Schierwagen, et al. focus on neuromorphological phenotyping in transgenic mice. 3D morphological data have been used to quantitatively characterize the morpholog-

ical phenotype of pyramidal neurons in transgenic mice. The authors calculated the multiscale fractal dimension (MFD) of reconstructed neuronal cells. Changes in the complexity of neuronal morphology due to permanent activation of p21Ras in the primary somatosensory cortex of transgenic mice correlate with changes in the MFD of dendrites of pyramidal neurons. Transgenic neurons seem slightly less complex (i.e., have lower peak fractal dimension) if compared with the wild type. On the other hand, it is shown that the enhanced p21Ras activity in transgenic mice may lead to greater variety in the cell morphological phenotype.

Gibson, et al. introduce a quantitative model of ATP-mediated calcium wave propagation in astrocyte networks. In the past, attention has mainly been focused on neurons and the role they play, both individually and as parts of networks, in the functioning of the brain and nervous system. However, glial cells outnumber neurons in the brain, and it is now becoming apparent that, far from just performing supportive and housekeeping tasks, they are also actively engaged in information processing and possibly even learning. Communication in glial cells is manifested by waves of calcium ions (Ca^{2+}) that are released from internal stores, and these waves are observed experimentally using fluorescent markers attached to the ions. The waves can be initiated by stimulation of a single cell, and initially it was assumed that the transmission mechanism involved the passage of an intercellular signalling agent through gap junctions connecting the cells. However, a surprising feature is that in many cases the calcium waves can cross cell-free zones, thus indicating the presence of an extracellular messenger. The authors have constructed a mathematical model of calcium wave propagation in networks of model astrocytes, these being a subclass of glial cells. The extracellular signalling agent is ATP (adenosine triphosphate), and it acts on metabotropic purinergic receptors on the astrocytes, initiating a G-protein cascade leading to the production of inositol trisphosphate (IP_3) and the subsequent release of Ca^{2+} from intracellular stores via IP_3-sensitive channels. Stimulation of one cell (by a pulse of ATP or by raising the IP_3 level) leads to the regenerative release of ATP both from this cell and from neighboring cells, and hence a Ca^{2+} wave. Results are given for the propagation of Ca^{2+} waves in two-dimensional arrays of model astrocytes and also in lanes with cell-free zones in between. These theoretical considerations support the concept of extracellular purinergic transmission in astrocyte networks.

Atay and Hutt analyze the dynamics of neural fields with distributed transmission speeds. In particular, the continuous field model of neural populations is considered with the addition of a distribution of transmission speeds. The speed distribution arises as a result of the natural variability of the properties of axons, such as their degree of myelination. The authors analyze the stability and bifurcations of equilibrium solutions for the resulting field dynamics. Using a perturbation approach, it is shown that the speed distribution affects the frequency of bifurcating periodic solutions and the phase speed of traveling waves. The theoretical findings are illustrated by numerical calculations.

Hampel focuses on the estimation of differential entropy for positive random variables and its application in computational neuroscience. This chapter takes essentials steps toward the goal of a differential entropy concept and provides a set of methods related to differential entropy estimation. At the beginning, the author defines the basic

terms: entropy, differential entropy, Kullback–Leibler distance, and refractory periods. Relations between differential entropy and the Kullback–Leibler distance are demonstrated. Hereafter a detailed description of the used methods is provided. These methods can be divided into three groups: parametric methods of entropy estimation, "plug-in" entropy estimators based on nonparametric density estimation, and direct entropy estimators. The formulas for direct entropy estimation based on the first four sample moments are introduced. The results are illustrated by comparison of the methods of entropy estimation, combined with two refractory period estimates. In particular, the author compares the estimates based on the histogram, the kernel density estimator, the sample spacing method, Vasicek's method, the nearest neighbor distance method, and the methods based on sample moments.

Tyrcha discusses the dynamics of integrate-and-fire models. In particular, a model for the generation of action potentials by a neuron is presented. This model is based on standard and commonly accepted properties of excitable cells (neurons). The novelty is that under quite natural assumptions the generation of action potentials is described as a special case of a general model for systems generating recurrent biological events. A formula for a density function of the membrane potential distribution in the firing times of the neuron is derived. An analysis of time intervals between spikes is of special interest. Three different interspike interval distributions are found, where one of them is close to the stable distribution. This is consistent with the known literature hypothesis that stable interspike intervals form part of the neural chain in which information is being preserved.

Kotti and Rigas present a Monte Carlo method for the identification of the muscle spindle. In particular, the behavior of the muscle spindle is described by using a logistic regression model. The system receives input from a motoneuron and fires through the Ia sensory axon that transfers the information to the spinal cord and from there to the brain. Three functions, which are of special interest, are included in the model: the threshold, the recovery, and the summation functions. The most favorable method of estimating the parameters of the muscle spindle is the maximum likelihood approach. However, there are cases when this approach fails to converge because some of the model's parameters are considered to be perfect predictors. In this case, the exact likelihood can be used, which succeeds in finding the estimates and the exact confidence intervals for the unknown parameters. This method has the main drawback that it is computationally very demanding, especially with large data sets. A good alternative in this case is a specific application of the Monte Carlo technique.

Marsalek and Drapal discuss mechanisms of coincidence detection in the auditory brainstem. The auditory brainstem in mammals contains a neural circuit for sound localization. The exact functioning of this circuit is still under controversy. Two spike generation mechanisms studied previously, excitatory coincidence detection and inhibitory coincidence detection, are studied here regarding the input-output relationship of the spike time densities. The authors propose that synchronous binary multiplication operation on spikes is the underlying process of these two variants of coincidence detection. A derivation of time to the spike is shown, which allows us to estimate the contribution of the neural circuit in the auditory brainstem to the overall reaction time of sound localization. The brainstem contribution is minute compared to the conduc-

tion delays in the mammalian neocortex. Finally, the skewness of the resulting output spike time densities is discussed in both the excitatory and inhibitory cases, and the inhibitory case is shown to be close to the normal density with a standard goodness-of-fit test for the normal probability density function.

Hübsch and Tittgemeyer present a multi-scale analysis of brain surface data. The human brain is characterized by complex convolution patterns. Analyzing the variability of these patterns among human subjects can reveal information for the detection of diseases that affect the human brain. This chapter presents a novel method to visualize the brain surface and its folding pattern at different scales. The analysis steps involve the transformation of the cortical surface from high resolution MRT images to an initial representation as a triangulated mesh, and finally to a representation as a series of spherical harmonic basis functions. The spherical harmonic parameterization of the surface is translation, rotation, and scaling invariant. The parametric representation gives a multidimensional coefficient vector for each cortical surface. The technique allows easier recognition of convolutional patterns. The method is a first step toward a statistical multi-scale analysis of the brain surface.

Scheper focuses on spike generation processes. Over the last years, the focus of the computational aspects of neurons has moved from synaptic weight and firing rate encoding to temporal firing encoding. On the other hand, several elements of these models have been based on some conceptual assumptions that imply relatively simple dynamic behavior of neuronal membrane activity in an active-passive process. In line with recent advances that yielded a better understanding of the biochemical processes that occur within cells, it is proposed that the processes that are involved in a membrane depolarization cascade are less static than has been assumed so far. In particular, the possibilities of low-level computation at the membrane level need to be explored more extensively. In this chapter some computational properties of the spike generation processes are explored using phenomenological models.

Part V focuses on innovative mathematical methods and education and consists of eight chapters.

Claussen introduces Offdiagonal Complexity (OdC) as a computationally quick network complexity measure and applies it to protein networks and cell division. Many complex biological, social, and economic networks show topologies drastically differing from random graphs. But what is a complex network, i.e., how can one quantify the complexity of a graph? Here the OdC, a new, and computationally cheap, measure of complexity is defined, based on the node-node link cross-distribution, whose nondiagonal elements characterize the graph structure beyond link distribution, cluster coefficient, and average path length. The OdC approach is applied to the *Helicobacter pylori* protein interaction network and randomly rewired surrogates thereof. In addition, OdC is used to characterize the spatial complexity of cell aggregates. The author investigates the earliest embryo development states of *Caenorhabditis elegans*. The development states of the premorphogenetic phase are represented by symmetric binary-valued cell connection matrices with dimension growing from 4 to 385. These matrices can be interpreted as adjacency matrices of an undirected graph or network. The OdC approach allows us to describe quantitatively the complexity of the cell aggregate geometry.

Simitev and Biktashev present an analytically solvable asymptotic model of atrial excitability. In particular, a three-variable simplified model of excitation fronts in human atrial tissue is introduced. The model is derived by novel asymptotic techniques from a previously introduced biophysically realistic model. An iterative analytical solution of the model is presented, which is in excellent quantitative agreement with the realistic model. This opens new possibilities for analytical studies as well as for efficient numerical simulation of this and other cardiac models of similar structure.

Lalam and Jacob introduce a Bayesian approach to the quantitative polymerase chain reaction. This reaction aims at determining the initial amount of a specific portion of DNA molecules from the observation of the amplification process of the DNA molecules' quantity. This amplification process is achieved through successive replication cycles and depends on the efficiency of the replication of the molecules. Modelling the amplification process by a branching process, the authors estimate the unknown parameter using Markov chain Monte Carlo methods under a Bayesian framework.

Buck-Sorlin, et al. present a model of poplar (*Populus* sp.) physiology and morphology based on relational growth grammars. Functional-structural plant models (FSPMs), combining the physiological function of a plant with its architecture, require precise and transparent specifications. This can be viewed as a new challenge to the design of programming languages. Here the authors introduce, exemplarily, a model of young poplar trees, based on the new formalism of relational growth grammars (RGGs), which extend the well-known Lindenmayer (L-)systems to a specific type of node- and edge-labelled graph grammars. The model has been written in the programming language XL, which extends standard Java by rule-based programming with RGGs and overcomes many of the disadvantages of L-systems. RGGs can bridge different scales: In the presented model, morphogenetic rules in L-system style are combined with rules describing a regulatory network of hormone biosynthesis and rules updating photosynthate concentrations of shoot modules, all in one and the same formalism.

Calvez and Dolak-Struß analyze the asymptotic behavior of a two-dimensional Keller–Segel model with and without density control. In particular, the authors study the Keller–Segel model for chemotaxis, consisting of a drift-diffusion equation describing the evolution of the cell density coupled to an equation for the chemoattractant. It is known that in the classical Keller–Segel model, solutions can become unbounded in finite time. The authors present recent analytical results for this model, and compare its behavior in two space dimensions numerically to the behavior of a model accounting for the finite volume of cells. This modified Keller–Segel model relies on the assumption that cells stop aggregating when their density is too high, and thus allows for the global existence of solutions. The authors characterize the slow movement of a certain class of plateau-shaped solutions and perform numerical experiments for both models, showing that solutions of the classical (before blow-up) and of the density control model share common features: regions of high cell density are attracted by each other and, under suitable boundary conditions, by the domain boundaries.

Jacob discusses saturation effects in population dynamics. The chapter deals with the behavior of a branching population undergoing saturation effects when it becomes too large. The author studies, in particular, the limits of the prediction given in the

setting of the deterministic dynamical system related to the stochastic branching process modelling the evolution of the population. Furthermore, *Jacob* also generalizes the usual Markovian branching processes of order one to size-dependent branching processes that may have a longer memory and gives conditions leading to an almost sure extinction of the process while the dynamical system is persistent. The notion of reproductive rate is explained and generalized. Finally, some examples are given, in particular, the amplification process in the PCR (polymerase chain reaction).

Klauß and Voß-Böhme consider modelling and simulation by stochastic interacting particle systems. Stochastic interacting particle systems (IPSs) are individual-based models, which include stochastic local interactions on a spatial lattice. In this respect an IPS works similarly to a cellular automaton. However, IPSs are continuous-time Markov processes, hence there is a large background of analytical methods. Furthermore, one has the possibility to simulate the system on a finite lattice. The authors explain the modelling steps and describe the core of a simulation algorithm. The idea is to convince the reader that IPSs can be used to set up and simulate sophisticated and applicable models, but allow an analytical approach as well.

De Vries and Hillen present mathematical biology teaching experiences from a summer school for undergraduates. For the past four years, the University of Alberta has hosted a summer school on mathematical biology, aimed at undergraduate students who have completed 2–3 years of study in mathematics or a similar quantitative science. The aim of this summer school is to introduce the students to mathematical modelling and analysis applied to real biological systems. In the span of 10 days, students attend lectures and exercise sessions, learn how to set up mathematical models, and use analytical and computational tools to relate them to biological data. Furthermore, they experience the modelling process by working on a research project. In this chapter, the authors explain their teaching philosophy, share some unique features of the summer school, and exemplify the key course components.

Finally, the volume owes its existence to the support of many colleagues. First of all, thanks go to the authors of the various contributions. We would also like to express our gratitude to the members of the ECMTB05 scientific committee and to a significant number of other colleagues for providing reviews and suggestions. ECMTB05 and these peer-reviewed proceedings have only become possible thanks to the strong institutional support provided by the Centre for Information Services and High Performance Computing (Technical University of Dresden). Particular thanks go to Professor Wolfgang E. Nagel, the head of this Centre and many colleagues at the Centre, particularly Niloy Ganguly, Christian Hoffmann, Samatha Kottha, Claudia Schmidt, Jörn Starruß, and Sabine Vollheim. Finally, we would like to thank Tom Grasso of Birkhäuser for making this project possible.

<div style="text-align: right">

Dresden, January 2007
Andreas Deutsch (for the editors)

</div>

Contents

Part III Immunology   **131**

Part IV Neural Systems and the Brain   **183**

Part I

Epidemiology

Could Low-Efficacy Malaria Vaccines Increase Secondary Infections in Endemic Areas?

Robert J. Smith?

Department of Mathematics and Faculty of Medicine, The University of Ottawa,
585 King Edward Ave, Ottawa, Ontario, K1N 6N5, Canada; rsmith43@uottawa.ca

Summary. Recent breakthroughs in malaria vaccines have given new hope that a safe, effective malaria vaccine may be found. The following epidemiological questions are addressed: 1. What level of vaccination coverage is required to offset the limitations of an imperfect disease-modifying vaccine? 2. Could the introduction of a low-efficacy malaria vaccine lead to an increase in the number of secondary infections? 3. What characteristics of such a vaccine will have the greatest effect on the outcome? A mathematical model is developed for a disease-modifying malaria vaccine that is given once prior to infection, and the minimum coverage level for disease eradication is established. There is a threshold depending on the relative rate of infection, the efficacy of the vaccine and the duration of infection. Vaccines which reduce the rate and duration of infection will always result in a decrease in secondary infections. More surprisingly, there is a duration "shoulder," such that vaccines that increase the duration of infection slightly will still lead to a decrease in secondary infections, even if the rate of infection is unchanged. Beyond this, the number of secondary infections will increase unless the rate of infection is sufficiently lowered. This is critical for low-efficacy vaccines.

Key words: Malaria, vaccines, coverage, rate of infection, duration of infection, efficacy.

1.1 Introduction

Malaria remains one of the most important human diseases throughout the tropical and subtropical regions of the world and causes more than 300 million acute illnesses and at least one million deaths annually [18]. 90% of deaths due to malaria occur in sub-Saharan Africa, mostly among young children [17]. The search for a malaria vaccine is now over seventy years old [6], and a great deal of effort and funding has been put into the task [11]. Recent vaccine findings [1] have renewed the interest in the potential role of vaccines within malaria-control programs by focusing on the possibility of an anti-malarial vaccine delivered to infants prior to infection.

In this chapter, a model of malaria infection is developed which combines the classic Aron models [2,3] with those of vaccine models [8], but includes disease-modifying effects based on theoretical HIV vaccine models [4, 15]. The following epidemiological questions are addressed: 1. What level of vaccination coverage is required to offset

the limitations of an imperfect disease-modifying vaccine? 2. Could the introduction of a low-efficacy malaria vaccine lead to an increase in the number of secondary infections? 3. What characteristics of such a vaccine will have the greatest effect on the outcome?

1.2 The Model

A malaria vaccine could have different potential effects, including (a) reducing mortality due to malaria, (b) increasing the recovery rate, (c) increasing the acquired immunity rate or d) reducing the rate of infection. Possible limitations of a vaccination program include (i) the vaccine may only be delivered to a proportion p of the population, (ii) the vaccine may only "take" in a proportion ϵ of people vaccinated, (iii) the vaccine may wane over time (ω is the rate of waning of immunity) and (iv) the vaccine may have a suboptimal efficacy ψ. It is assumed that all vaccinated individuals are vaccinated before infection, reflecting the situation in [1]. Furthermore, unlike in HIV models (but in common with other models of vaccination; eg pertussis [16]), the vaccine may wane before, during or after infection.

It follows that *"successfully vaccinated"* individuals consist of those who received the vaccine, for whom the vaccine "took" and for whom the vaccine did not wane prior to infection. All other individuals shall be referred to as *unprotected individuals*, regardless of whether they received the vaccine or not, since the net effect prior to infection is identical. (See [4] and [15] for more detailed discussions.) Note that "successfully vaccinated" individuals have the potential to become infected (if the vaccine efficacy ψ is less than 100%, or if vaccine-induced immunity wanes subsequently) and cause secondary infections. These individuals may have a reduced rate of infection, but will have an increased life expectancy. They may recover faster from the disease and their disease-induced mortality will be lower. Consequently, their total duration of infection may either decrease (due to higher recovery rates) or increase (due to fewer deaths from infection).

It can be assumed that mosquitos are either susceptible (M) or infected (N), have birth rate Ω and that their death rate (μ_M) does not vary significantly if they are infected. Individuals who have experienced infection may recover (without substantial gain in immunity) at *recovery rate* h_k ($k = U, V$; U = unvaccinated, V = vaccinated) or may become temporarily immune at *acquired immunity rate* α_k ($k = U, V$). See [5,9,10,12] for further details. Temporarily immune individuals will become susceptible again at rate δ_k ($k = U, V$). The rate of infection of an infected individual in class X_k is β_k ($k = U, V$) and the rate of infecting a mosquito is β_M (assumed identical from either class of individual, since mosquitos are not vaccinated). The birth rate is π, the background death rate is μ and γ_k is the death rate due to malaria ($k = U, V$). Thus, the model is

$$\frac{dM}{dt} = \Omega - \beta_M Y_U M - \beta_M Y_V M - \mu_M M$$

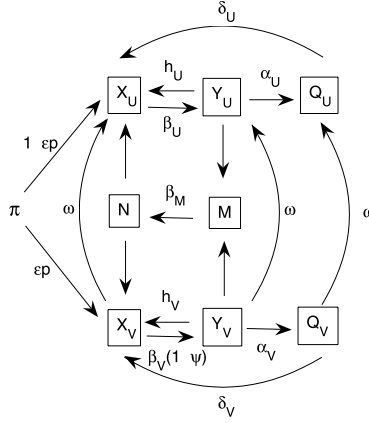$$\frac{dN}{dt} = \beta_M Y_U M + \beta_M Y_V M - \mu_M N$$

Fig. 1.1. Schematic representation of the model, representing both unprotected and "successfully vaccinated" individuals, as well as mosquitos. The background mortalities for humans μ (in all compartments) and mosquitos μ_M (in both compartments), as well as disease-induced mortality for humans γ_U, γ_V (in the infected compartments) are not drawn in, for conciseness.

$$\frac{dX_U}{dt} = (1 - \epsilon p)\pi - \mu X_U - \beta_U N X_U + \omega X_V + h_U Y_U + \delta_U Q_U$$

$$\frac{dX_V}{dt} = \epsilon p\pi - \mu X_V - (1 - \psi)\beta_V N X_V - \omega X_V + h_V Y_V + \delta_V Q_V$$

$$\frac{dY_U}{dt} = \beta_U N X_U - (\mu + \gamma_U + \alpha_U + h_U)Y_U + \omega Y_V$$

$$\frac{dY_V}{dt} = (1 - \psi)\beta_V X_V - (\mu + \gamma_V + \alpha_V + h_V)Y_V - \omega Y_V$$

$$\frac{dQ_U}{dt} = \alpha_U Y_U - (\mu + \delta_U)Q_U + \omega Q_V$$

$$\frac{dQ_V}{dt} = \alpha_V Y_V - (\mu + \delta_V)Q_V - \omega Q_V .$$

The model is illustrated in Fig. 1.1.

With the notation $\xi_k = \mu + \gamma_k + \alpha_k + h_k$ $(k = U, V)$, $1/\xi_K$ is the total duration of the infectious period for unprotected and "successfully vaccinated" individuals, respectively. It is expected that the recovery rates α_V, h_V will increase due to the vaccine, but that the disease-induced death rate γ_V will decrease. It follows that the total duration of the infectious period for vaccinated individuals may either increase or decrease. It is also expected that the rate of infection β_V will not increase.

1.3 Analysis

The disease-free equilibrium satisfies $\bar{M} = \Omega/\mu_M$, $\bar{X}_U = [\pi(\mu(1 - \epsilon p) + \omega)]/[\mu(\mu + \omega)]$, $\bar{X}_V = \epsilon p\pi/(\mu + \omega)$ and $\bar{N} = \bar{Y}_U = \bar{Y}_V = \bar{Q}_U = \bar{Q}_V = 0$.

Thus, the proportion of the population that is successfully vaccinated, S, satisfies $S = \bar{X}_V/(\bar{X}_U + \bar{X}_V) = \epsilon p \mu/(\mu + \omega)$. In particular, $\bar{X}_U = (\pi/\mu)(1 - S)$ and $\bar{X}_V = (\pi/\mu)S$.

At the disease-free equilibrium, the Jacobian matrix is $J =$

$$
\begin{bmatrix}
\mu_M & 0 & 0 & 0 & -\beta_M\bar{M} & -\beta_M\bar{M} & 0 & 0 \\
0 & -\mu_M & 0 & 0 & \beta_M\bar{M} & \beta_M\bar{M} & 0 & 0 \\
0 & -\beta_U\bar{X}_U & -\mu & \omega & h_U & 0 & \delta_U & 0 \\
0 & -(1-\psi)\beta_V\bar{X}_V & 0 & -\mu-\omega & 0 & h_V & 0 & \delta_V \\
0 & \beta_U\bar{X}_U & 0 & 0 & -\xi_U & \omega & 0 & 0 \\
0 & (1-\psi)\beta_U\bar{X}_V & 0 & 0 & 0 & -\xi_V-\omega & 0 & 0 \\
0 & 0 & 0 & 0 & \alpha_U & 0 & -\mu-\delta_U & \omega \\
0 & 0 & 0 & 0 & 0 & \alpha_V & 0 & -\mu-\delta_V-\omega
\end{bmatrix}.
$$

Thus, $\det(J - \Lambda I) = -(\mu_M + \Lambda)(\mu + \Lambda)(\mu + \omega + \Lambda)(\mu + \delta_U + \Lambda)(\mu + \delta_V + \omega + \Lambda)\det M$, where

$$
M = \begin{bmatrix}
-\mu_M - \Lambda & \beta_M\bar{M} & \beta_M\bar{M} \\
\beta_U\bar{X}_U & -\xi_U - \Lambda & \omega \\
(1-\psi)\beta_V\bar{X}_V & 0 & -\xi_V - \omega - \Lambda
\end{bmatrix}.
$$

Thus, the largest eigenvalue for J will be the largest eigenvalue for M. The vanishing determinant condition gives $-\mu_M\xi_U(\xi_V + \omega) + (1 - \psi)\beta_V\beta_M\omega\bar{X}_V\bar{M} + (1 - \psi)\xi_U\beta_V\beta_M\bar{X}_V\bar{M} + (\xi_V + \omega)\beta_U\beta_M\bar{X}_U\bar{M} = 0$. Hence,

$$
\frac{(1-\psi)\beta_V\beta_M\bar{M}(\xi_U + \omega)}{\mu_M\xi_U(\xi_V + \omega)}\bar{X}_V + \frac{\beta_U\beta_M\bar{M}}{\mu_M\xi_U}\bar{X}_U = 1 .
$$

Individuals who are vaccinated with disease-modifying vaccines have the potential to become infected and cause secondary infections. Such individuals may have a reduced rate of infection, but will have an increased survival time. The reproduction number in a population with vaccination is R_V, in contrast to R_0, the basic reproduction number in an unvaccinated population.

If there is no vaccine, $S = 0$, so $\bar{X}_V = 0$, $\bar{X}_U = \pi/\mu$ and hence the vanishing determinant condition gives $R_0 = \pi\Omega\beta_U\beta_M/\mu\mu_M^2\xi_U$. If the entire population is successfully vaccinated, $S = 1$ and $\omega = 0$, so $\bar{X}_V = \pi/\mu$, $\bar{X}_U = 0$ and hence the vanishing determinant condition gives $R_V = (1 - \psi)(\pi\Omega\beta_V\beta_M/\mu\mu_M^2\xi_V)$. Thus, the population reproduction number is $R_P = (1 - S)R_0 + SR_V$. See [4,7,13–15].

To estimate the minimum coverage levels p_c for an imperfect disease-modifying vaccine, when $R_P = 1$, this last equation can be rearranged to produce

$$
S = \frac{\epsilon p_c\mu}{\mu + \omega} = \frac{1 - R_0}{R_V - R_0} .
$$

Thus, the threshold disease-modifying vaccine coverage level is

$$
p_c = \frac{(\mu + \omega)(\mu + \gamma_V + \alpha_V + h_V)[\mu\mu_M^2(\mu + \gamma_U + \alpha_U + h_U) - \beta_U\beta_M\Omega\pi]}{\epsilon\mu\beta_M\Omega\pi[(1 - \psi)\beta_V(\mu + \gamma_U + \alpha_U + h_U) - \beta_U(\mu + \gamma_V + \alpha_V + h_V)]} . \quad (1.1)
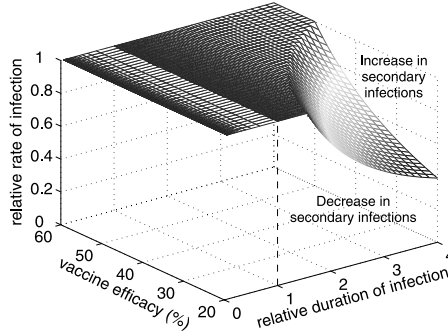$$

Fig. 1.2. The relationship between the relative rate of infection, the relative duration of infection and the vaccine efficacy. A disease-modifying vaccine which reduces the duration of infection will always lead to a decrease in secondary infections, regardless of the efficacy of the vaccine. More surprisingly, a vaccine which increases the duration of infection can still result in an overall decrease in secondary infections, but the outcome depends on the rate of infection and the efficacy of the vaccine. There is a duration "shoulder," such that vaccines that increase the duration of infection slightly will still result in a net decrease in secondary infections. However, as the duration of infection increases, the number of secondary infections will increase, unless the rate of infection is lowered accordingly. This is critical for low-efficacy vaccines.

Vaccination programs whose coverage levels exceed this proportion of the population are likely to eradicate the disease.

Once a vaccine is introduced, the number of secondary infections will increase if $R_P > R_0$ (i.e., if the population reproduction number after the introduction of a vaccine is greater than the reproduction number currently). This occurs when

$$(1 - S)R_0 + SR_V > R_0$$
$$\frac{\beta_V}{\beta_U} > \frac{\xi_V}{(1 - \psi)^2 \xi_U} \,.$$

This is illustrated in Fig. 1.2.

Clearly, if the rate of infection and the duration of infection both decrease, then there will always be a decrease in the number of secondary infections. More surprisingly, for a given efficacy of the vaccine, there is a duration "shoulder," such that a small increase in the duration of infection will still decrease the number of secondary infections, even if the rate of infection is unchanged. However, if the duration of infection is increased beyond this shoulder, then it is crucial that the rate of infection be decreased accordingly. This is critical for low-efficacy vaccines.

The "shoulder" occurs when the relative duration of infection satisfies

$$\frac{1/\xi_V}{1/\xi_U} = \frac{1}{(1 - \psi)^2}$$

for a given vaccine efficacy ψ. For example, a 20% efficacious vaccine could accommodate an increase in the duration of infection by as much as 1.5625 times the current

duration of infection, with no reduction in the rate of infection and still result in a decrease in secondary infections. However, a 20% efficacious vaccine that increased the duration of infection by a factor of 4 would lead to an increase in secondary infections unless the rate of infection for the vaccinated population were reduced to 40% of the current rate of infection.

1.4 Discussion

A vaccination program implementing a disease-modifying malaria vaccine in an endemic area should have a minimum coverage level p_c, as estimated by (1.1). If the proportion of the population that can be vaccinated exceeds p_c, then such a vaccination program is likely to result in the eradication of the disease.

Furthermore, reducing the transmission probability of such a disease-modifying vaccine is crucial, for vaccines whose duration of infection increases significantly. While it is expected that a disease-modifying vaccine would increase the recovery rates, it would also decrease the rate of disease-induced mortality, so the total duration of the infectious period for a vaccinated individual may either increase or decrease. If this duration decreases, then the number of secondary infections will always decrease, regardless of the vaccine efficacy, so long as the rate of infection does not increase.

There is a duration "shoulder," such that the number of secondary infections will always decrease if the duration increases within this shoulder. However, an increase beyond the "shoulder" will lead to an increase in secondary infections, unless the rate of infection of the vaccine is lowered accordingly. This is critical for low-efficacy vaccines.

It should be noted that these results primarily apply to areas in which malaria is endemic. A disease-modifying malaria vaccine with a high duration of infection (for example, one which drastically reduced disease-induced mortality, but which had negligible effect on the recovery rates) might be quite desirable for a temporary outbreak of malaria in the developed world, if the prospect of reinfection is negligible. In endemic areas however, such a vaccine would likely make the situation worse. It follows that low-efficacy vaccines which result in high durations of infection but which do not significantly lower the rate of infection should not be used in endemic areas.

Acknowledgments

References

1. Alonso, P. L., Sacarlal, J., Aponte, J. J., Leach, A., Macete, E., Milman, J., Mandomando, I., Spiessens, B., Guinovart, C., Espasa, M., Bassat, Q., Aide, P., Ofori-Anyinam, O., Navia, M.

M., Corachan, S., Ceuppens, M., Dubois, M. C., Demoitie, M. A., Dubovsky, F., Menendez, C., Tornieporth, N., Ballou, W. R., Thompson, R., Cohen, J.: Efficacy of the RTS,S/AS02A vaccine against *Plasmodium falciparum* infection and disease in young African children: randomised controlled trial. Lancet, **364**, 1411–20 (2004).

2. Aron, J. L.: Mathematical modeling of immunity to malaria. Math. Biosci., **90**, 385–396 (1988).

3. Aron, J. L., May, R. M.: The population dynamics of malaria. In: Anderson, R.M. (ed) *The Population Dynamics of Infectious Diseases: Theory and Applications*. Chapman & Hall, London (1982).

4. Blower, S. M., Koelle, K., Mills, J.: Health Policy Modeling: Epidemic Control, HIV Vaccines and Risky Behavior. In: Kaplan, E., Brookmeyer, R. (eds) *Quantitative Evaluation of HIV Prevention Programs*. Yale University Press, New Haven, CT (2002).

5. Boyd, M. F. (ed): *Malariology, Saunders*, Philadelphia (1949).

6. Desowitz, R. S.: *Federal Bodysnatchers and the New Guinea Virus: Tales of Parasites, People and Politics*. W.W. Norton & Company, New York (2002).

7. Heffernan, J. M., Smith, R. J., Wahl, L. M.: Perspectives on the basic reproductive ratio. J. R. Soc. Interface, **2**, 281–293 (2005).

8. Koella, J.: On the use of mathematical models of malaria transmission. Acta Trop., **49**, 1–25 (1991).

9. Mackinnon, M. J., Read, A. F.: The effects of host immunity on virulence-transmissibility relationship in the rodent malaria parasite *Plasmodium chabaudi*. Parasitology, **126**, 103–112 (2003).

10. Molineaux, L., Gramiccia, G.: *The Garki Project: Research on the Epidemiology and Control of Malaria in the Sudan Savannah of West Africa*. World Health Organization, Geneva (1980).

11. Moorthy, V. S., Good, M. F., Hill, A. V.: Malaria vaccine developments. Lancet., **363**, 150–6 (2004).

12. Pérignon, J. L., Druilhe, P.: Immune mechanisms underlying the premunition against *Plasmodium falciparum* malaria. Mem. Inst. Oswaldo Cruz, Rio de Janeiro, **89**, Suppl. II (1994).

13. Porco, T. C., Blower, S. M.: Designing HIV vaccination policies: Subtypes and cross-immunity. Interfaces, **28**, 167–190 (1998).

14. Porco, T. C., Blower, S. M.: HIV vaccines: The effect of the mode of action on the coexistence of HIV subtypes. Math. Pop. Studies, **8**, 205–229 (2000).

15. Smith, R. J., Blower, S. M.: Could disease-modifying HIV vaccines cause population-level perversity? Lancet Inf. Dis., **4**, 636–639 (2004).

16. van Boven, M., de Melker, H. E., Schellekens, J. F., Kretzschmar, M.: Waning immunity and sub-clinical infection in an epidemic model: Implications for pertussis in The Netherlands. Math Biosci., **164**, 161–82 (2000).

17. van de Perre, P., Dedet, J.-P.: Vaccine efficacy: winning a battle (not war) against malaria. Lancet, **364**, 1411–1420 (2004).

18. World Health Organisation, Roll Back Malaria infosheet: What is Malaria? http://malaria.who.int/cmc_upload/0/000/015/372/RBMInfosheet_1.htm (accessed 26 May 2007).

Modeling of the Invasion of a Fungal Disease over a Vineyard

Jean-Baptiste Burie,[1] Agnès Calonnec,[2] and Michel Langlais[1]

[1] UMR CNRS 5466, Mathématiques Appliquées de Bordeaux, INRIA futurs, Equipe Anubis, case 26, Université Victor Segalen Bordeaux 2, 146 rue Léo Saignat, 33076 Bordeaux Cedex, France; burie@sm.u-bordeaux2.fr
[2] INRA-CR de Bordeaux, UMR INRA-ENITA en Santé végétale, BP 81, 33883 Villenave d'Ornon, France; calonnec@bordeaux.inra.fr

Summary. The spatiotemporal spreading of a fungal disease over a vineyard is investigated using a susceptible-exposed-infected-removed (SEIR)-type model coupled with a set of partial differential equations describing the dispersal of the spores. The model takes into account both short and long range dispersal of spores and growth of the foliar surface. Results of numerical simulations are presented. A mathematical result for the asymptotic behavior of the solutions is given as well.

Key words: SEIR model, dispersal, diffusion, large time behavior.

2.1 Introduction

Integrated pest management offers an attractive alternative to routine chemical application by treating only in response to disease risk indicators. Powdery mildew, caused by the fungus *Uncinula necator*, is the most economically important and widespread disease of grapevines. For this disease, the main factor of risk is a timing of the attack early in the season combined with the phenological stage of the host. The leaves are the first to be infected, and there is a spatial relationship between maps of frequency of leaves diseased early in the season with maps of frequency of bunches with high severity [4,8]. A better knowledge of the mechanisms of the disease propagation could help to improve its control at the plot scale by tailoring treatments to local specific needs, or at the estate scale by treating only specific plots.

We aim at building a mathematical model of this fungal epidemic with a particular stress on the dispersal mechanism of the spores produced by the colonies of fungus. Already much work has been done on the subject of dispersal for various kinds of dispersers such as animals, seeds and spores (see, e.g., [6,10,11] and references therein).

In particular, we want to investigate the role of a dual dispersal mechanism in which the spores produced may either disperse inside the vine stock and germinate near the colony (short range dispersal) or may be lifted up above the vine rows and fall far from the colony (long range dispersal).

Our goal is to build a model which is a simpler version, and consequently easier to analyse, of a much more elaborate one [5]. This latter model couples a mechanistic model for the growth of each vine stock in the vineyard with a dispersal model using ray-tracing-like techniques at the vine stock scale and a distribution law at the vineyard scale for the spores escaping the vine stock.

In [13], the authors considered a two-dimensional (2D) spatial model based upon such a dual dispersal mechanism using diffusion theory coupled with a Vanderplank equation [12]. Using this Vanderplank equation leads to delay equations that complexify the mathematical analysis of the model. Instead, in this chapter, we will use a susceptible, exposed, infectious, removed (SEIR) compartmental model as used in classical epidemiology (see, e.g., [1,3]) to take into account the local extension of the disease. In the nonspatial case, a comparison between these two approaches can be found in [9].

During an epidemic lasting a whole season from bud break until grape maturation, the growth of the host cannot be neglected. We include a description of the host growth in our model. We also take into consideration the specific spatial organisation of vineyards that are made of several separate rows.

This chapter is organised as follows. After having described the model, we perform a mathematical analysis and present numerical simulations.

2.2 The Model

The vectors of a fungal disease are the spores produced by the colonies of fungus that lie on the vegetal tissue, which may be leaves, buds, fruits, etc. We assume for simplicity that the time variation of the surface of a colony can be neglected. Then as in [9] we consider the unit of disease to be a colony and the host to be a site, that is the surface occupied by a colony.

The cycle of the epidemic is as follows: when spores fall upon the vegetal tissue, they may create a new colony which will produce spores after some latency period and during some sporulating period.

Let Ω be a regular 2D spatial domain. Let t be the time and let x denote the position of some point in Ω. We will use the following notation for the state variables.

As in the case of a SEIR model, the total density N of sites susceptible to host a colony of fungus at (x, t) is subdivided into healthy H, latent L, sporulating I and removed (postinfectious) R.

We want to devise a model that takes into account multiple ranges of dispersal for the spores in order to investigate their different roles for the spreading of the epidemic. Spores may disperse separately or as infection units (packages of spores). For simplicity, we only take into account two ranges for dispersal: a short range (spores disperse inside the vine stock where they come from), and a longer range (spores disperse at the vineyard scale). Let $S(x, t)$ denote the density of spores produced by the colonies. The spores' total density S is subdivided acccording to the range of dispersal; the short range dispersal spore density S_1 and the longer range one S_2. They are produced by a

sporulating colony with rate $r_p > 0$ and may disperse at short range with a constant probability $F \in [0, 1]$ and at longer range with probability $(1 - F)$.

We assume that the spores disperse according to a diffusion process with Fickian diffusion coefficient $D_1 > 0$ (short range) or $D_2 > D_1 > 0$ (longer range) as in [13]. Using Fickian diffusion for long range dispersal may seem unrealistic at first. But the spores are not necessarily taken away along dominating wind directions. The dispersal is also due to turbulence that provides the energy to tear off the spores from the leaves.

Spores fall upon the vineyard with some deposition rate $\delta_1 > 0$ or $\delta_2 > 0$; we will set $\delta_1 = \delta_2$ in the numerical simulations. We thus find the first set of equations of our model that describes the production of spores by the colonies and their dispersal:

$$
\begin{cases}
\frac{\partial S_1}{\partial t}(x, t) = \nabla. (D_1 \nabla S_1(x, t)) - \delta_1 S_1(x, t) + r_p F I(x, t) \\
\\
\frac{\partial S_2}{\partial t}(x, t) = \nabla. (D_2 \nabla S_2(x, t)) - \delta_2 S_2(x, t) + r_p (1 - F) I(x, t)
\end{cases}
\tag{2.1}
$$

for $x \in \Omega$ and $t > 0$.

Moreover, we assume that no spores come from outside the vineyard. The spores produced by the fungus colonies should freely escape from the vineyard. To simulate this, we choose a computing domain Ω with vine rows located at the center and surrounded by a region with no vines. Then, if Ω is large enough with respect to diffusion coefficients, spores do not reach the boundary and their densities at these points should be equal to 0. Thus, we impose Dirichlet conditions on the boundary

$$
S_1(x, t) = S_2(x, t) = 0 \text{ for } x \in \partial\Omega \text{ and } t > 0.
\tag{2.2}
$$

We also set nonnegative initial conditions

$$
S_1(x, 0) = S_1^0(x) \geq 0, \; S_2(x, 0) = S_2^0(x) \geq 0 \text{ for } x \in \Omega.
\tag{2.3}
$$

Let $\Omega_r \subset \Omega$ denote the area covered by the vine rows. We devise our model in such a way that for all $t > 0$ and $x \in \Omega$, $N(x, t)$ equals 0 if $x \notin \Omega_r$.

The powdery mildew epidemic has no impact upon the growth of the host. This growth brings new sites available for colonization. We study the epidemic during one single season; then we assume that the time variation of the total number of colony sites inside the rows obeys a logistic law

$$
\frac{\partial N}{\partial t}(x, t) = r N(x, t) \left(1 - \frac{N(x, t)}{K}\right), \text{ for } x \in \Omega_r,
\tag{2.4}
$$

where $r > 0$ is the growth rate and $K > 0$ the carrying capacity. Although r and K are constant for simplicity, we could introduce spatial heterogeneities for the host growth assuming r and K depend on x. Provided r, K are bounded, our results can be easily extended to handle this.

Next, the local evolution of the disease at some point $x \in \Omega_r$ (inside a row) obeys the classical SEIR model, whereas we set $N(x, t) = L(x, t) = I(x, t) = R(x, t) = 0$ for $t \geq 0$ if $x \notin \Omega_r$. Let p and i denote the mean duration of the latency and infectious period respectively. Let E be the inoculum effectiveness (probability for the spores to

succeed in creating a new colony upon a site). Taking into account (2.4), this yields the second set of equations of our model for $x \in \Omega_r$:

$$
\begin{cases}
\frac{\partial H}{\partial t}(x, t) = -E(\delta_1 S_1(x, t) + \delta_2 S_2(x, t))\frac{H(x,t)}{N(x,t)} + rN(x, t)\left(1 - \frac{N(x,t)}{K}\right) \\[2mm]
\frac{\partial L}{\partial t}(x, t) = +E(\delta_1 S_1(x, t) + \delta_2 S_2(x, t))\frac{H(x,t)}{N(x,t)} - \frac{1}{p}L(x, t) \\[2mm]
\frac{\partial I}{\partial t}(x, t) = +\frac{1}{p}L(x, t) - \frac{1}{i}I(x, t) \\[2mm]
\frac{\partial R}{\partial t}(x, t) = +\frac{1}{i}I(x, t)
\end{cases}
\tag{2.5}
$$

supplemented with nonnegative initial conditions

$$
H(x, 0) = H^0(x) \geq 0, \ L(x, 0) = L^0(x) \geq 0,
$$
$$
I(x, 0) = I^0(x) \geq 0, \ R(x, 0) = R^0(x) \geq 0 \text{ for } x \in \Omega_r
\tag{2.6}
$$

The contact term in (2.5) is based upon a proportionate mixing assumption. Though our model includes host growth, this assumption is in agreement with the underlying hypothesis of classical epidemiologic models in phytopathology (see Vanderplank [12]) that states that the rate of increase of diseased tissue is proportional to the amount of spores multiplied by the probability that these spores fall upon healthy tissues. A similar approach for including host growth in a model of phytopathology but with nonspatial delay equations can be found in [2].

2.3 Theoretical Results

We have the following existence result for our model.

Theorem 1 *The system (2.1),(2.5) is well posed: let H^0, L^0, I^0, R^0 be in $L^\infty(\Omega)$ and S_1^0, S_2^0 be in $L^2(\Omega)$; the system posseses a unique componentwise nonnegative solution that exists globally in time.*

The proof of this theorem follows standard arguments (see, e.g., [7]) and will not be detailed here.

The large time behavior of the solutions can be described as follows.

Theorem 2 *If the hypothesis of the previous existence theorem is satisfied, then as t goes to infinity, $S_1(x, t)$ and $S_2(x, t)$ converge to 0 in the $L^2(\Omega)$ and $H_0^1(\Omega)$ norms. And there are nonnegative functions H_∞ and R_∞ such that for all $x \in \Omega_r$, $H^\infty(x) + R^\infty(x) = K$ and*

$$
\lim_{t \to +\infty} H(x, t) = H_\infty(x)
$$
$$
\lim_{t \to +\infty} L(x, t) = \lim_{t \to +\infty} I(x, t) = 0
$$
$$
\lim_{t \to +\infty} R(x, t) = R_\infty(x).
$$